J|A|C|S COMMUNICATIONS

Published on Web 03/12/2009

Oleylamine-Mediated Synthesis of Pd Nanoparticles for Catalytic Formic Acid Oxidation

Vismadeb Mazumder and Shouheng Sun*

Department of Chemistry, Brown University, Providence, Rhode Island 02912

Received January 21, 2009; E-mail: ssun@brown.edu

The need to limit Pt usage in catalysis, especially in fuel cell reactions, has promoted the search for non-Pt nanoparticle (NP) catalysts with comparable catalytic properties.[1] Among the metal-based catalysts studied to date, Pd is a promising alternative. Like Pt, Pd also catalyzes myriad chemical reactions. Recent progress in Pd catalysis has revealed that Pd in NP forms can catalyze the oxidation of formic acid at the anode of polymer electrolyte membrane fuel cells (PEMFCs) with greater resistance to CO than Pt catalysts.[2] Studies of this oxidation process have indicated that while the Pd(100) planes are more active, the (111) planes are less susceptible to oxidation and have a lower peak potential,[3] making these (111)-faceted Pd catalysts more practical for fuel cell applications. In numerous solution-phase syntheses of monodisperse Pd NPs, trialkylphosphines, 1-alkanethiols, or polymer molecules such as RNA or polyvinylpyrrolidone (PVP) have been applied to stabilize Pd NP dispersions.[4] In particular, a variety of Pd NPs of different shapes have been synthesized by a modified polyol reduction process in the presence of ethylene glycol and PVP.[5] A common feature of all these syntheses is the presence of bulky or strongly binding surfactants around these Pd NPs to prevent their aggregation. Although quite a few of these Pd NPs can be made with very narrow size and shape distributions, they have very limited catalytic activities because of the lack of a "clean", surfactant-free NP surface.

Here we report an oleylamine-mediated synthesis of monodisperse Pd NPs for catalytic oxidation of formic acid under fuel cell reaction conditions. The previously identified problem associated with the low catalytic activity of high-quality Pd NPs originates from the presence of a polymeric surfactant or strong chemical bonds of the surfactant on the Pd NP surface. An obvious solution is to use a weakly binding surfactant to stabilize Pd NPs during the synthesis and purification process. Once the Pd NPs are anchored on a solid support, this surfactant can be readily removed, leaving a clean NP surface for catalytic evaluation. Recently, Au NPs were synthesized by reducing $HAuCl_4$ in tetralin in the presence of oleylamine and borane tributylamine complex (BTB).[6] Further experiments indicated that pure oleylamine could be used as a solvent, surfactant, and reducing agent for making Au and FePt nanowires.[7] By combining the chemistry of these two methods, we have succeeded in synthesizing monodisperse Pd NPs by reducing $Pd(acac)_2$ (acac = acetylacetonate) with oleylamine and BTB. We have found that these oleylamine-coated Pd NPs can be readily "cleaned" by acetic acid washing, leaving a sufficiently large electrochemically active surface area (ECASA). They were catalytically active for formic acid oxidation in 0.1 M $HClO_4$ solution and showed little decrease in activity after 1500 cyclic volammetric cycles. The reported synthesis offers a general approach to highly active and stable Pd nanocatalysts for potential fuel cell applications.

The 4.5 nm Pd NPs were synthesized by the reduction of $Pd(acac)_2$ in oleylamine and BTB. Here oleylamine acted as the solvent, surfactant, and reductant, and BTB served as a coreductant. In the synthesis, $Pd(acac)_2$ was first dissolved in 15 mL of oleylamine, and the solution was heated to 60 °C. BTB in 3 mL of oleylamine was injected into the heated solution, leading to an instant color change in the reaction mixture from colorless to black-brown. Next, the resulting solution was heated at 90 °C for 1 h and then cooled to room temperature for NP separation.[8] Figure 1A shows a transmission electron microscopy (TEM) image of the 4.5 nm Pd NPs obtained from the synthesis. The NPs have a narrow size distribution with a standard deviation of ~8% in the diameter. A high-resolution TEM (HRTEM) study of a series of single Pd NPs showed that each NP has a polycrystalline structure (Figure 1B). The crystal domains within each Pd NP have an interfringe distance of 0.23 nm, which is close to the lattice spacing of the (111) planes of the face-centered cubic (fcc) Pd crystal (0.223 nm). The polycrystalline structure of the NPs was further confirmed by the X-ray diffraction pattern of the Pd NP assembly (Figure S1 in the Supporting Information), from which the average NP size was estimated to be ~3.5 nm, which is smaller than the value of 4.5 nm measured from the TEM images in Figure 1A,B.

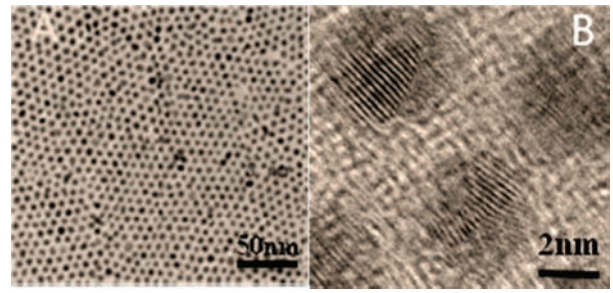

Figure 1. (A) TEM and (B) HRTEM images of the 4.5 nm Pd NPs prepared by the reduction of $Pd(acac)_2$ in oleylamine and BTB.

Of the three Pd precursors [$Pd(acac)_2$, $Pd(NO_3)_2$, and Na_2PdCl_4] screened under the described synthetic conditions, $Pd(acac)_2$ empirically gave the best-quality Pd NPs. The NP growth seemed to follow the Ostwald ripening process, as the TEM image of the sample taken from the reaction mixture 15 min after BTB injection contained ~3 nm Pd NPs, which were easily isolated and characterized (Figure S2). These NPs further grew into 4.5 nm Pd NPs after 60 min at 90 °C. Increasing the reaction time beyond 90 min did not lead to larger NPs. The use of another alkylamine, such as dodecylamine, hexadecylamine, or octadecylamine, instead of oleylamine in the synthesis did not provide high-quality NPs. It seems that the double bond present in oleylamine plays a critical role in Pd NP stabilization and growth with a narrow size distribution. However, oleylamine alone cannot be used to make monodisperse Pd NPs. The weak reducing power offered by oleylamine prolongs the reduction process, causing multinucleation and an uneven growth rate over differently sized Pd nuclei. BTB fared better than other borane reductants we tested, such as borane−morpholine complex and $NaBH_4$. It offers an ideal combination with oleylamine for the facile synthesis of monodisperse Pd NPs, and boron does not associate with Pd NPs, as proven by inductively coupled plasma mass

10.1021/ja9004915 CCC: $40.75

spectrometry (ICP-MS) analysis. The process has been extended to the synthesis of 3 nm Pt NPs (Figure S3).

The catalytic activity of the 4.5 nm Pd NPs toward formic acid oxidation was evaluated in an electrochemical measurement system[8] and compared with that of a commercial Pd on carbon (commercial Pd/C) catalyst (Sigma-Aldrich 205699). To prepare our 4.5 nm Pd/C nanocatalyst, we mixed and stirred a hexane dispersion of 10 mg of Pd NPs with an equal amount of Ketjen carbon (surface area 800 m^2/g) for 2 h, after which hexane was evaporated from the solution. The Pd/C catalyst was then immersed in 99% acetic acid for 10 h to remove oleylamine from the Pd NPs. The catalyst was washed with ethanol, dried under vacuum, and characterized by energy dispersive absorption X-ray (EDAX) spectroscopy (Figure S4)[9] and TEM. An appropriate amount of deionized water was added to the treated Pd/C catalyst, and the mixture was stirred for 1 h to form a 2 mg/mL suspension. The TEM image of the 4.5 nm Pd/C catalyst in Figure 2A shows that the acetic acid wash did not degrade the quality of the NPs on the C support and that the Pd NPs were well-dispersed over the support surface with greater retention of the NP characteristics than obtained using the annealing techniques we tested (Figure S5). A 20 μL aliquot of the Pd/C suspension was placed on a glassy carbon working electrode and dried under vacuum. The catalyst was fixed on the electrode by depositing a layer of 0.1% Nafion. Ag/AgCl and Pt wire were used as reference and counter electrodes, respectively.

The electrodes were immersed in 0.1 M $HClO_4$ solution (308 K) under constant nitrogen bubbling, and the potential was scanned from −0.25 to 1.0 V (vs normal hydrogen electrode, NHE) at a scan rate 50 mV/s to obtain the cyclic voltammograms (CVs) of both our 4.5 nm Pd/C and the commercial Pd/C catalysts (Figure S6). These CVs were used to estimate the ECASA of the catalysts by a calculation of the hydrogen desorption area of the catalysts.[10] The peak at 0.4 V seen for the commercial Pd/C catalyst represents oxidation on the Pd surface and is characteristic of the presence of (100) peaks (Figure S7).[11] The calculated ECASA for the 4.5 nm Pd/C catalyst (182 cm^2) was ∼40% greater than that of the commercial Pd/C catalyst (129 cm^2).

In the presence of 2 M formic acid at a scan rate of 10 mV/s, the 4.5 nm Pd/C catalyst showed a peak potential of 0.4 V (Figure 2B), similar to the observations made with single-crystalline Pd(111) electrodes.[3] The commercial Pd/C catalyst's activity was retarded by the formation of a Pd oxide layer, and its peak potential was 0.7 V.[12] Efficient reduction of the Pd oxide layer from the Pd surface activates the rate of formic acid oxidation on polycrystalline Pd electrodes because the Pd atoms are not at equilibrium with their own crystal lattice.[13] The 4.5 nm Pd/C catalyst removes the oxide layer efficiently, as seen by the sharp peak at 0.65 V in the negative scan. This explains the nearly 2-fold gain of our 4.5 nm Pd/C catalyst relative to the commercial Pd/C catalyst, both in peak potential and maximum current density (J) at 0.4 V.

Redox reactions on the surface of catalysts often cause major catalyst degradations, leading to a loss of activity.[14] Stability tests on the two Pd/C catalysts were carried out under the same conditions as in the CV measurements, barring the use of ambient conditions. The ECASA of the 4.5 nm Pd/C catalyst was measured to be 152 cm^2 after 1500 CV cycles (Figure S8). This 16% drop leads to no drastic changes in its $J-E$ characteristics (Figure 2C). For the commercial Pd/C catalyst, however, the ECASA was reduced to 40 cm^2 (a drop of ∼69% from 129 cm^2) after the stability test (Figure S9), and its $J-E$ curve displayed a major loss in activity (Figure S10). Under anodic oxidation conditions in the acidic medium, the loss of stability generally stems from the tendency of NPs to coagulate over time (1500 CV cycles, ∼12 h). While the profile of our 4.5 nm Pd/C NPs showed some degradation

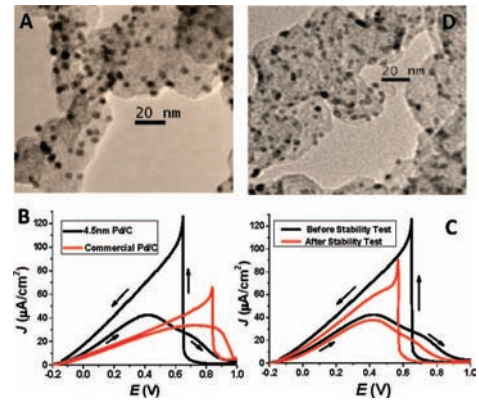

Figure 2. (A) TEM image of the 4.5 nm Pd/C catalyst. (B) Specific activity of formic acid oxidation of the catalyst shown in (A) and the commercial Pd/C catalyst. (C) Specific activity of formic acid oxidation of the 4.5 nm Pd/C before and after the stability test. (D) TEM image of the 4.5 nm Pd/C catalyst after the stability test.

(Figure 2D), the commercial catalyst was completely disfigured (Figure S11). This proves that our monodispersed Pd NPs are efficiently attached to the Ketjen carbon support and are thus a more active and stable catalyst for formic acid oxidation.

We have reported here a facile synthesis of monodisperse Pd NPs by the reduction of $Pd(acac)_2$ with oleylamine and BTB. The oleylamine-coated Pd NPs are readily "cleaned" by an acetic acid wash, and the Pd NPs supported on Ketjen carbon are catalytically active and stable for formic acid oxidation in $HClO_4$ solution. We are currently developing similar syntheses and evaluating various highly active non-Pt catalysts for fuel cell applications.

Acknowledgment. This work was supported by NSF/DMR 0606264 and the Brown seed fund.

Supporting Information Available: Pd nanoparticle synthesis and characterization and the results of electrochemical studies. This material is available free of charge via the Internet at http://pubs.acs.org.

References

(1) Wang, B. *J. Power Sources* **2005**, *152*, 1–15.
(2) Larsen, R.; Ha, S.; Zakzeski, J.; Masel, R. I. *J. Power Sources* **2006**, *157*, 78–84.
(3) Baldauf, M.; Kolb, D. M. *J. Phys. Chem.* **1996**, *100*, 11375–11381.
(4) (a) Kim, S. W.; Park, J.; Jang, Y.; Chung, Y.; Hwang, S.; Hyeon, T. *Nano Lett.* **2003**, *3*, 1289–1291. (b) Gugliotti, L. A.; Feldheim, D. L.; Eaton, B. E. *Science* **2004**, *304*, 850–852. (c) Zheng, N.; Fan, J.; Stucky, G. D. *J. Am. Chem. Soc.* **2006**, *128*, 6550–6551. (d) Xiong, Y.; Chen, J.; Wiley, B.; Xia, Y. *J. Am. Chem. Soc.* **2005**, *127*, 7332–7333.
(5) Xiong, Y.; Xia, Y. *Adv. Mater.* **2007**, *19*, 3385–3391.
(6) Peng, S.; Lee, Y.; Wang, C.; Yin, H.; Dai, S.; Sun, S. *Nano Res.* **2008**, *1*, 229–234.
(7) (a) Wang, C.; Hu, Y.; Lieber, C. M.; Sun, S. *J. Am. Chem. Soc.* **2008**, *130*, 8902–8903. (b) Wang, C.; Hou, Y.; Kim, J.; Sun, S. *Angew. Chem., Int. Ed.* **2007**, *46*, 6333–6335.
(8) See the Supporting Information.
(9) As a model study to check the efficiency of the acetic acid treatment, we attached the Pd NPs to a commercial silica (SiO_2) support and washed the Pd/SiO_2 with acetic acid under the same conditions as for the 4.5 nm Pd/C catalyst. Figure S4 shows the EDAX spectra of the Pd/SiO_2 before and after the acetic acid treatment. The carbon−nitrogen peak at 0.2 keV disappeared after the wash, indicating that oleylamine is efficiently removed from the Pd/SiO_2 moiety by acetic acid.
(10) Woods, R. In *Elecroanalytical Chemistry*; Bard, A. J., Ed.; Marcel Dekker: New York, 1976; Vol. 9, p 176.
(11) Hoshi, N.; Noma, M.; Suzuki, T.; Hori, Y. *J. Electroanal. Chem.* **1997**, *421*, 15–18.
(12) Hoshi, N.; Kida, K.; Nakamura, M.; Nakada, M.; Osada, K. *J. Phys. Chem. B* **2006**, *110*, 12480–12484.
(13) Manzanares, M. I.; Pavese, A. G.; Solis, V. M. *J. Electroanal. Chem.* **1991**, *310*, 159–167.
(14) Gasteiger, H. A.; Kocha, S. S.; Sompalli, B.; Wagner, F. T. *Appl. Catal., B* **2005**, *56*, 9–35.

JA9004915